Hindawi
Journal of Chemistry
Volume 2020, Article ID 8403940, 10 pages
https://doi.org/10.1155/2020/8403940

Research Article

Effects of Ethanol Blending on the Formation of Soot in *n*-Heptane/Air Coflow Diffusion Flame

Yuchen Ya,[1] Xiaokang Nie,[1] Licheng Peng,[2] Longkai Xiang,[1] Jialong Hu,[1] Wenlong Dong,[1] and Huaqiang Chu[1]

[1]*School of Energy and Environment, Anhui University of Technology, Ma'anshan 243002, Anhui, China*
[2]*College of Ecology and Environment, Hainan University, Haikou 570228, Hainan, China*

Correspondence should be addressed to Huaqiang Chu; hqchust@163.com

Received 17 November 2019; Revised 20 January 2020; Accepted 29 January 2020; Published 26 March 2020

Guest Editor: Yaojie Tu

Laminar diffusion flame was used to study the effect of ethanol on *n*-heptane flame in terms of the morphology and microstructure of soot under atomization combustion. For the same carbon mass flux at the outlet of the burner, the ratio of ethanol doping in *n*-heptane was changed, and the soot was collected from the axial positions of the flame at different heights using the thermophoresis probe method. The results showed that the flame height increased significantly with the increasing ratio of ethanol doping. When the ratio of ethanol and *n*-heptane (C_E/C_N) was 1.5, the flame height increased by 10 mm compared with that of pure *n*-heptane flame. Besides, the temperature in the center of the flame decreased with the increasing ratio of ethanol doping, but the temperature in the low position was higher than that in the pure *n*-heptane flame, and the temperature in the high position was lower than that in the pure *n*-heptane flame. However, the flame temperature was the highest when the proportion of ethanol in the mixture was greater than that of *n*-heptane. The temperature at the flame center decreased with the increasing ratio of ethanol doping, while the temperature at the flame edge increased with the ratio. The primary particle size of soot (soot size hereafter) in all working conditions increased with the increase of flame height, which was in line with the general growth law of soot. Moreover, the soot size at the same height decreased with the increasing ratio of ethanol doping, and this trend was most obvious at the flame height of 20 mm and 30 mm. Compared with pure *n*-heptane, when C_E/C_N was 1.5, the soot size at 20 mm and 30 mm decreased by an average of 34.83%, indicating that ethanol could inhibit the surface growth of soot particle. Furthermore, the density of soot particles collected by a single copper net decreased significantly, indicating that ethanol could reduce the production amount of soot.

1. Introduction

The problem of air pollution has plagued humans for many years. Currently, soot particles are generally considered to be the main cause of atmospheric particulate pollution. They usually come from incomplete combustion of hydrocarbon fuels, which can generate energy waste, resulting in global warming, environmental pollution, and diseases [1–4]. Thus, how to improve the fuel combustion efficiency and reduce the emission of pollutants is a hot issue. Alcohols, as the important liquid fuels, are composed of hydrocarbyl and hydroxyl (OH), which are readily available biomass liquid fuels in industry, and it is known that the hydroxyl can promote the combustion process and reduce the emission of soot particle. Moreover, the high vaporization latent heat of alcohols can reduce the maximal combustion temperature and inhibit the formation of NOx. Under such circumstances, methanol and ethanol are often used as fuel additives [5]. Extensive research has demonstrated that oxygen-containing fuel is an effective technique to reduce the carbon emission of diesel engine. For instance, ethanol has been successfully used in gasoline engines by blending with other fuels [6, 7]. Hamdam and Jubran [8] investigated the effect of ethanol addition on the gasoline combustion performance in engine. The results showed

that the optimal engine performance was reached when 5% ethanol was mixed with gasoline, and the fuel thermal efficiency was improved by 4% at low speed and 20% at high speed. Aharon et al. [9] conducted a weight reduction combustion experiment on droplet forming of *n*-heptane when being mixed with methanol or ethanol. They found that the combustion rate decreased dramatically with the increase of the initial droplet diameter in the air, and the effect of methanol and ethanol addition on combustion rate is not obvious. Moreover, Fan et al. [10] measured the ignition delay time of *n*-heptane/iso-octane/ethanol mixture and established a calculation model. Their results showed that the low temperature chemical inertness of ethanol extended the range of octane sensitivity. In the combustion process, the oxygen part of ethanol replaces O_2, and eventually the mole fraction of O_2 increases with the increasing ratio of ethanol [11]. Other studies demonstrated two ethanol/*n*-heptane mixture oxidation schemes through experiments and simulations [12] and modeled the chemical kinetics of the detailed scheme [13] and its simplified version [14].

In addition to the importance of increasing acetaldehyde yield through CH_3CHOH oxidation in ethanol/*n*-heptane mixtures of different proportions, a very similar oxidation pathway was found. Ergut et al. [15] investigated the generation of polycyclic aromatic hydrocarbons (PAHs) in ethylbenzene and ethanol flame at atmosphere pressure and pointed out that the generation rate of PAHs of ethanol was low even under lean oxygen combustion. Previous studies investigated the influence of ethanol doping ratio on the flame structure of *n*-heptane/ethanol and the formation rate of soot precursor [16]. It was found that the dehydrogenation rate of *n*-heptane was faster than that of ethanol, while ethanol promotes the reaction by providing active free radicals.

Oxygen-containing fuels with different structures would play different role in reducing soot emission, even in the same oxygen content [17]. Three methods are applied in the reduction of soot emission from alcohol: dilution, that is, reducing the aromatic hydrocarbon content of the fuel; oxygenation, through reducing the equivalence ratio and the number of carbon atoms that can be used to generate PAHs and soot; promotion of mixing effect, to lower the cetane number and prolong the stagnation period. It is an interesting finding that the presence of methanol and ethanol in ethylene diffusion flames had opposite effects on PAHs and soot formation in nonpremixed ethylene flame [18]. The dilution effect of methanol and the increased concentration of H_2 from the decomposition of methanol inhibit the formation of the initial benzene ring and the subsequent growth of PAHs and soot. On the contrary, the addition of a small amount of ethanol will promote the formation of soot. Zhang et al. [19] studied the effects of addition of dimethyl ether and ethanol on the formation of polycyclic aromatic hydrocarbons (PAHs) in premixed ethylene flame, and they found that C_2H_2 plays a key role in the formation of new aromatic rings. In addition, the nanostructure of soot particles is also a key to understand the properties of soot; not only is it related to the reactivity of soot [20] and the aromatic structure characteristics of soot surface [21–25], but also it has a certain relationship with carbon nanomaterials [26, 27].

Currently, there are quite limited studies regarding the effects of ethanol on the combustion flame of macromolecular hydrocarbon fuels, the growth process of soot in flames, and the change of soot morphology. The single component or mixture of *n*-heptane is often studied as an alternative to fuel oil [28]. The primary pyrolysis products of *n*-heptane are mainly methane, ethane, ethylene, propane, propylene, *n*-butane, 1-butene, 1-hexene, etc. [29]. With the increase of flame temperature, the secondary reaction of pyrolysis products increases, resulting in the increase of soot precursors and the final generation of a large amount of soot [30]. It is generally considered that cycloalkanes, cycloalkenes, and aromatic hydrocarbons are the main soot precursors [31]. The reaction becomes more complicated when ethanol is added, and this would change the groups of substances in the flame. Ethanol molecules contain hydroxyl groups, which are more likely to form active oxygen-containing intermediates during combustion, such as HCCO, CHO, and active OH radicals [32]. The increasing concentration of these components is beneficial to the reduction of the concentration of CH_3 and C_2H_2, for example, reducing the probability of the formation of PAHs through methylation cyclization and dehydrogenation plus acetylene and reducing the peak production of PAHs such as benzopyrene and naphthalene. Thus, soot particles cannot absorb more PAHs to form large diameter soot particles, which can inhibit the surface growth of soot, reduce the production of soot, promote the oxidation of basic carbon particles, and reduce the production of soot as well [33]. In this paper, the effects of ethanol on the change of soot particle size and nanostructure of *n*-heptane atomized flame and soot formation process were studied by mixing ethanol with *n*-heptane in different proportions.

2. Experimental Setup and Methods

The coaxial jet diffused flame experimental setup was used in this study, as shown in Figure 1, which mainly includes burner, flow control device, thermoprobe sampling system, and temperature detection system. In addition, liquid atomizer and insulation belt are also equipped for liquid fuel atomization. Gülder burner is widely used for the study of hydrocarbon fuel coaxial jet diffusion flame. More details about the burner can be found in our previous works [34, 35].

The mixed fuel is vaporized through an evaporator, and a stable laminar diffusion flame is formed when the oxidizer (air) is 60 L/min. High purity (>99%) *n*-heptane and ethanol were used for experiments, which were bought from Shanghai Aladdin Biochemical Technology Co., Ltd. The well-mixed fuel passes through the liquid flow controller and then through the evaporator, which has a liquid inlet and a diluent gas inlet. With nitrogen being a carrier of liquid fuel, the liquid dispersed and diluted, and then the mixture would

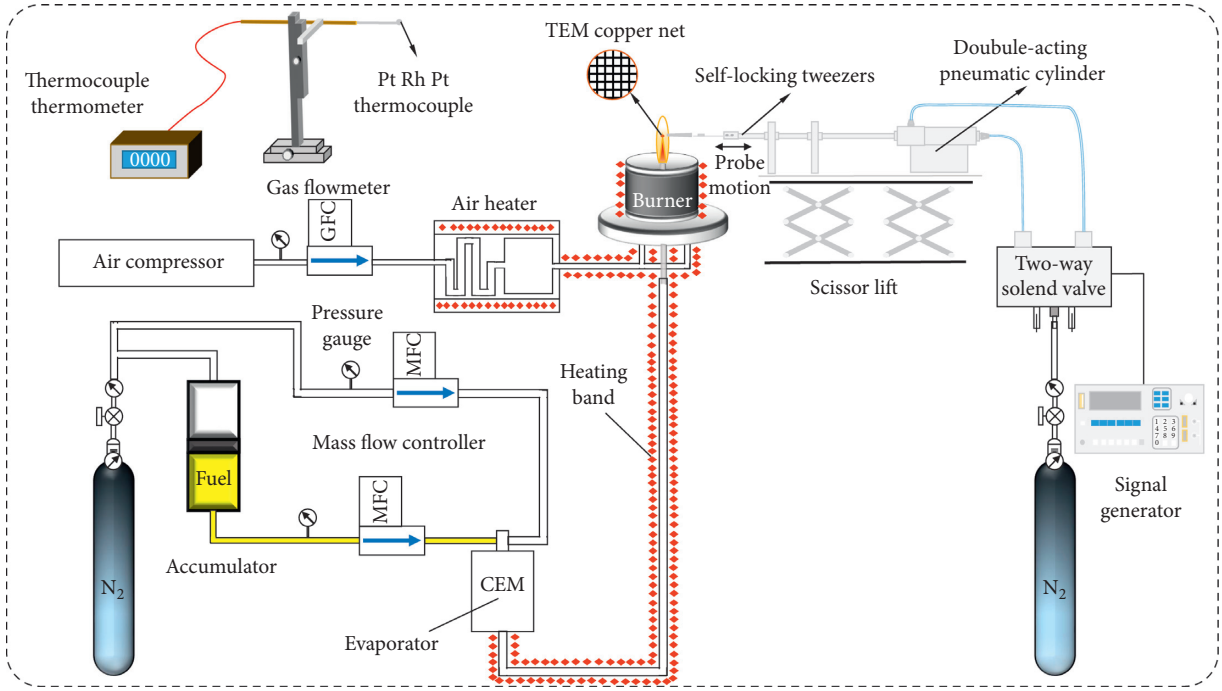

FIGURE 1: Schematic diagram of liquid fuel evaporative atomization combustion experiment system.

be vaporized in the evaporator. In this experiment, the evaporation temperature is 423.5 K, and the fuel is controlled by liquid flowmeter in the liquid atomizer. Finally, it passes through the insulated pipe, and then the laminar diffusion flame is formed in the nozzle. Besides, compressed dry air was used as the oxidizer (air) in this experiment.

In this paper, a CCD camera was used to record the shape of the flame. The soot samples were collected using a thermophoresis probe in the center of the flame, at different positions and heights. High resolution transmission electron microscopy (HRTEM, JEM-2100F) was used for detection, and the primary particle morphology and nanostructure of the soot were obtained by software statistics. The experimental conditions are shown in Table 1, ethanol and *n*-heptane mixed by volume fraction.

3. Results and Discussion

3.1. Comparison of Height for the Different Flames. The laminar diffusion flames of different ethanol addition on *n*-heptane are shown in Figure 2. The results showed that the flame extended distance in the air increased with the increasing proportion of ethanol in the fuel and mixed gas flow rate in the nozzle. For instance, the flame height increases with the increase of ethanol blending ratio, and the corresponding flame height reached up to 43 mm, 47 mm, 49 mm, and 53 mm when the ratio of C_E/C_N was maintained at 0, 1/4, 2/3, and 3/2, respectively. Additionally, the particle size of the droplet increases with the total liquid flow rate if a stable nitrogen flow rate is maintained; the combustion will require longer cracking time, and therefore, the combustion speed would be delayed. The results conform to the previous study [9].

The range of the low-temperature area (darker part) of the flame becomes wider with increasing ethanol doping ratio, and this may be attributed to the fact that the ethanol has high vaporization latent heat which can reduce the maximum combustion temperature. Since the hexadecane value of ethanol is low (8–10), mixing ethanol with *n*-heptane results in longer ignition delay and longer preparation time for ignition experience [36, 37]. Then, the fuel does not oxidized sufficiently at the initial position of the flame; while the cold zone widens in the flame, and the contour inside the flame becomes blurred through the flame image, and the edge between the low temperature area and the high temperature area becomes not obvious. This can be explained as follows. On the one hand, the increase in the amount of ethanol doping ratio requires that the pyrolysis of the fuel needs to absorb more heat and lower the temperature. On the other hand, the increase in the amount of ethanol doping ratio complicates the components in the flame. Ethanol pyrolysis and combustion increase the concentration of CH_2O, C_2H_4O, CO_2, H_2O, HCCO, CHO, and active OH radicals in the flames [38]. Moreover, the specific heat capacity of CO_2 and H_2O is relatively large, and this would cause the decrease of temperature below the flame and result in insignificant heat radiation [39].

Figure 3 shows the temperature comparison diagram of different flames at different heights (high above the burner, HAB). The distribution of flame temperature distribution under different working conditions was measured using the three-dimensional thermocouple temperature measuring device. The temperature of flame center increases with flame height. The temperature at the same height of flame firstly increases and then decreases along the flame center to the edge. Furthermore, the temperature at the flame edge at the

Table 1: Experimental conditions under different equivalence ratios of ethanol/*n*-heptane.

Cases	Ethanol: *n*-heptane (C_E/C_N)	Liquid flow (mg/min)	Nitrogen gas flow (mL/min)	Flame height (mm)
Case 1	0 : 1	150	250	43
Case 2	1 : 4	175	250	47
Case 3	2 : 3	210	250	49
Case 4	3 : 2	260	250	53

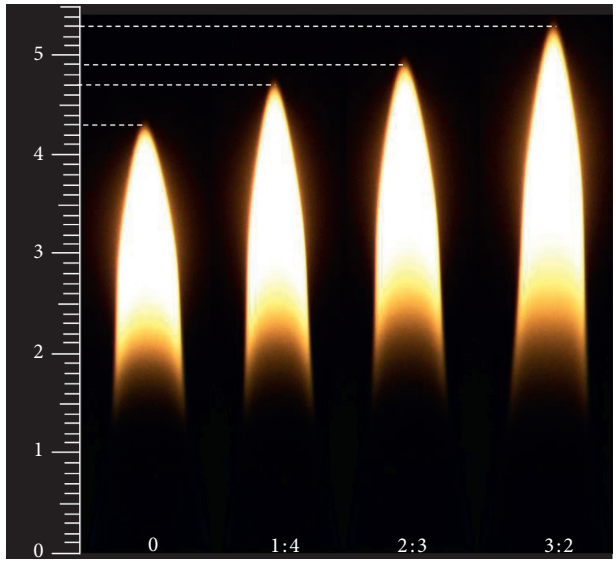

Figure 2: Still pictures of *n*-heptane mixed with different amounts of ethanol.

same height increases moderately with the increase of ethanol doping ratio. There are three reasons accounting for this: (1) The *n*-hexadecane value of ethanol is much lower than that of *n*-heptane, and the fuel has a longer lag period, so the initial flame temperature at the lower and center of the flame will be lower than that of the pure *n*-heptane flame. (2) The latent heat of ethanol vaporization is high, and meanwhile ethanol vaporization will absorb more heat at the lower and center part of the flame, so the temperature of the flame center will be lower. At a higher and the edge position of the flame, the full combustion of the fuel makes the ethanol completely vaporized and the temperature of the flame increases consequently. (3) The blending of ethanol increases the oxygen concentration and the amount of CO_2 and H_2O, resulting in a higher temperature at the edge of the flame and a lower highest temperature.

3.2. Comparison of Soot in the Different Flames. Figure 4 shows the HRTEM image of pure heptane and $C_E/C_N = 1.5$ at the center of the flame at different heights, with a magnification of 4×10^4 times. At the initial stage of combustion (HAB = 20 mm), some single carbon nuclei appear in the pure *n*-heptane diffusion flame, and their number density is very low. Single carbon nuclei collided as flame height increased to HAB = 30 mm, the surface growth of soot particles intensified, and PAHs cluster condensation was observed [40]. The soot particles gradually become regular spherical, the contour is clear, the particle size keeps increasing, and the flame height increases. The change in the particle size is mainly caused by the deposition and growth of PAHs on the surface of particles based on the dehydrogenation and carbonization mechanism, as well as the condensation and agglomeration between particles [41]. The carbonization degree of the soot particles was further strengthened with the increasing temperature in the flame center, and the particles continued to grow and condensate on the surface. Moreover, the oxidation was gradually strengthened, and the aggregates of particles in the soot increased, with an increase in overall size. At HAB = 40 mm, oxidation was further enhanced.

Under the action of Van der Waals force and Brownian force, the aggregates were further agglomerated to form chain shaped aggregate particles, the overall structure became loose, and the particle size of soot became smaller. Oxidation reaction exists in various development stages of nucleation, growth, coagulation, agglomeration, and oxidation of soot particles [42, 43]. In the lower position of the flame, the diffusion effect of oxygen is weak, and the surface growth of the soot particles is dominant, with increasing amount and size of soot particles. Furthermore, oxidation reaction gradually becomes the dominant factor with the continuous rise of the flame height, and the diameter of the soot particles gradually decreases. Near the flame tip, the oxidation reaction is very intense due to the high temperature in the flame center, and then the soot agglomerates would be quickly depleted and consumed accordingly. The

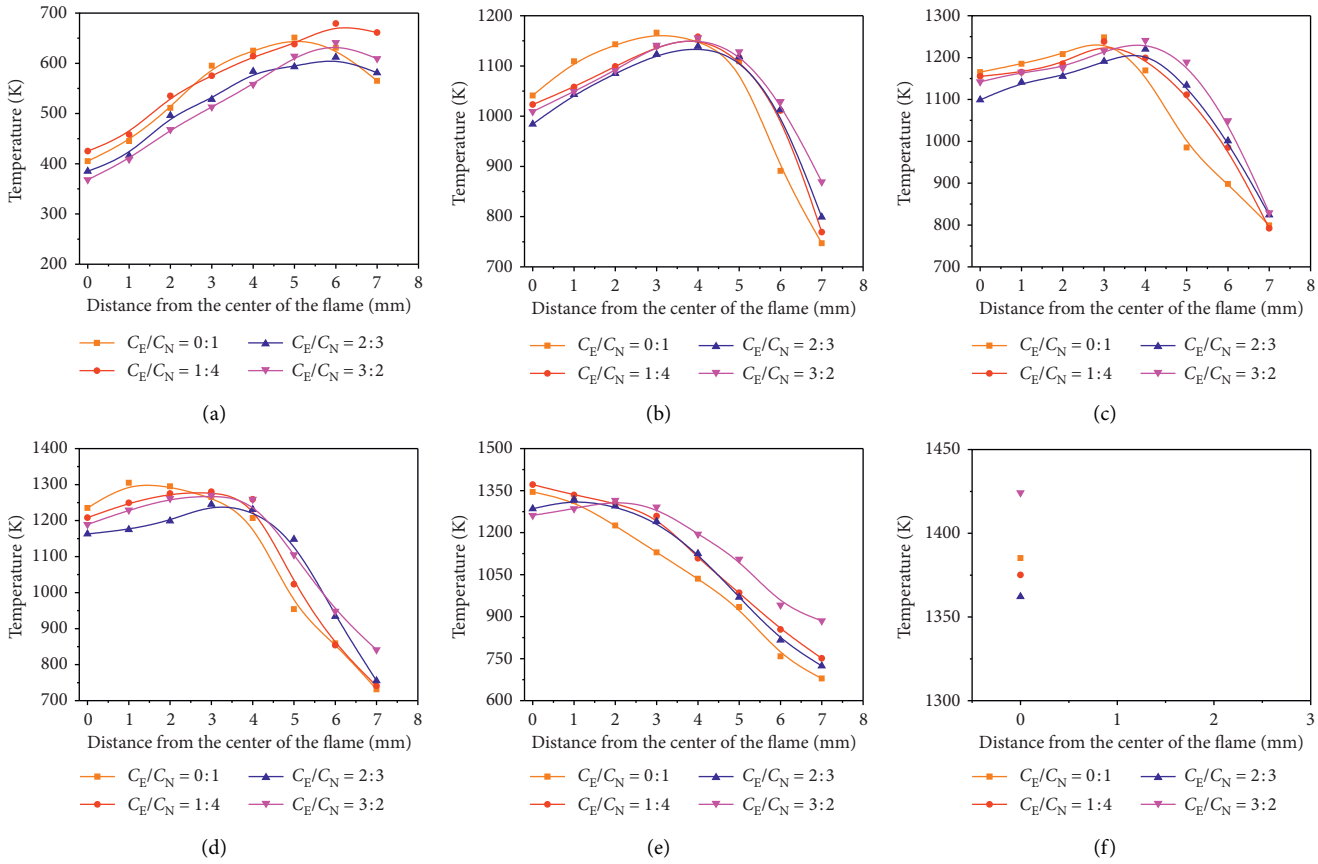

Figure 3: Temperature distribution of flame under different experimental conditions at the same height. (a) HAB = 0 cm. (b) HAB = 1 cm. (c) HAB = 2 cm. (d) HAB = 3 cm. (e) HAB = 4 cm. (f) Highest flame position.

fitting results indicated that the size of soot particles at different heights meets normal distribution, which was similar to the soot size range (e.g. 10~40 nm) of *n*-heptane in the previous studies [44, 45].

The growth process of soot along the axial height at the center of the diffused flame when C_E/C_N is 1/4 and 2/3, respectively, as shown in Figure 5, which is similar to pure *n*-heptane ($C_E/C_N = 0$). In other words, the development of soot particles has gone through five stages of nucleation, growth, condensation, agglomeration, and oxidation. The difference is that with the addition of ethanol, the surface of the soot at the same height growth is inhibited, the soot size becomes smaller, the agglomeration is delayed, and the oxidation reaction is advanced. Thus, the distribution of the initial soot particles in the sampled copper net at the lower position of the flame disperses. In other words, the gas-phase reaction area generated by soot in the flame is expanded, and the particle agglomeration oxidation area is decreased.

3.3. Analysis of the Distribution of Soot Sizes. The HRTEM images of soot particles in a laminar diffusion flame of *n*-heptane blended with ethanol are shown in Figure 6. The size of primary soot particles was measured using nanometer analysis software. Various images were taken at various flame heights for statistical calculation. The number of statistical particles was about 100, and the particle diameter distribution was nonlinearly fitted using LogNormal. Figure 7 gave the soot size under experimental conditions.

According to the statistical results of particle size, the soot size increases with the flame height. The soot particles varied dramatically with the flame height; e.g., HAB values of 20 mm, 30 mm, and 40 mm are given in Table 2. It can be seen that the soot size has a good regularity with the blending ratio of ethanol; i.e., the particle size obviously decreases with the ethanol doping ratio, except for $C_E/C_N = 0$ at HAB = 40 mm. The reason may be that the soot particles at the tip of the pure *n*-heptane flame were oxidized, resulting in a smaller particle size.

Compared with the soot size at $C_E/C_N = 0$ and $C_E/C_N = 3/2$, the flame height at HAB = 20 mm and HAB = 30 mm decreases by 33.16% and 36.47%. The trend was not obvious at HAB = 40 mm, and the soot size in the pure *n*-heptane flame was smaller than that in the flame with ethanol. This may be explained as follows: The soot particles matured along the radial position of the flame and were finally oxidized at the flame edge and tip with higher temperature. However, the blending of ethanol will

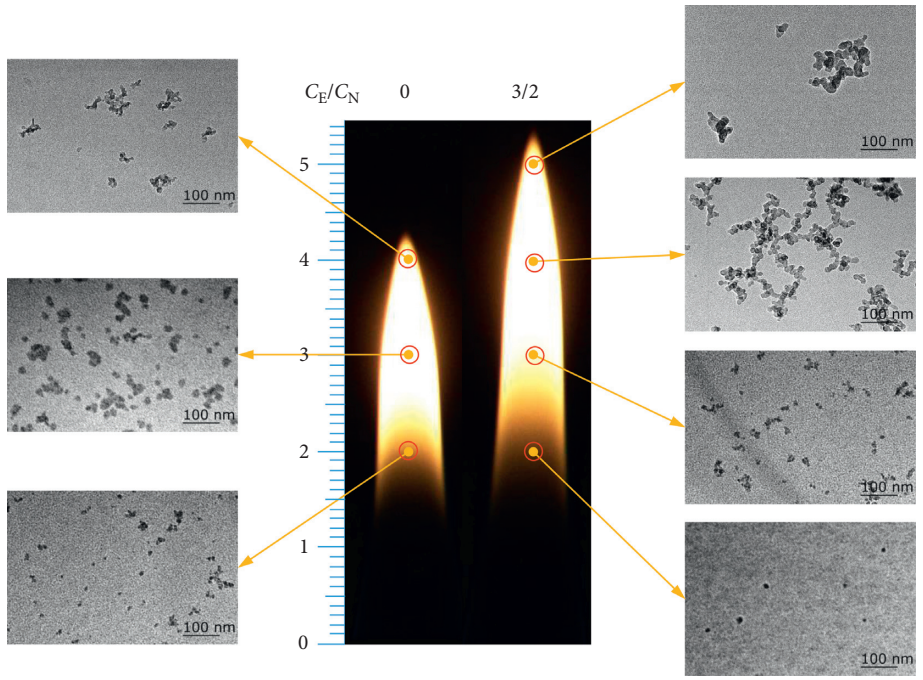

Figure 4: Comparison of soot morphology evolution of pure *n*-heptane and $C_E/C_N = 1.5$ in the laminar diffusion flame.

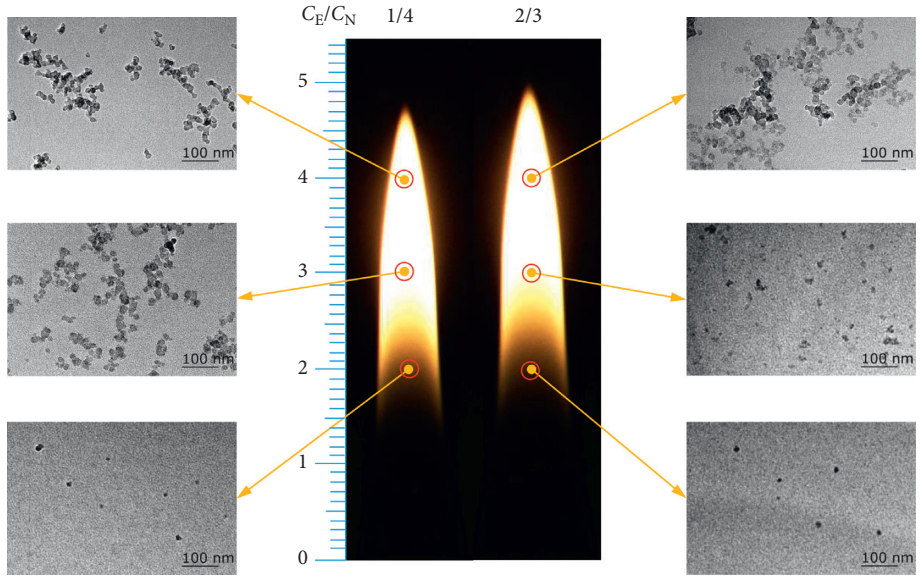

Figure 5: Comparison of soot morphology evolution of $C_E/C_N = 1/4$ and 2/3 in the laminar diffusion flame.

increase the flame height and decrease the maximum flame temperature, thus delaying the oxidation of soot. On the whole, the mechanism explaining the fact that soot particles decrease with the blending of ethanol is that ethanol molecules contain hydroxyl groups while ethanol contains 34.8% oxygen. Thus, some oxygen-containing intermediate radicals may be evolved in the combustion, which further promoted the oxidation of basic carbon particles. In addition, particle size is also affected by fuel and the flow rate of oxidizer, since the change in their initial velocity will affect the combustion reaction and the time of the soot particles staying in the flame [16]. Increasing the velocity of the oxidizer can suppress the energy transfer from the annular region producing soot to the flame axis. As the initial air velocity increases, it takes longer for soot to form at the flame axis, and the particle size of soot decreases with the increase of oxidizer velocity, which is the result of coagulation, surface growth reaction, and shorter residence time of fuel pyrolysis products [46]. As the increasing ratio of ethanol doping, the effects of ethanol on fuel dilution, oxidation, retardation of combustion period, and radiation of decomposition products would be enhanced, the size of the basic carbon particles moves toward the small particle diameter direction, and therefore the distribution range becomes narrow.

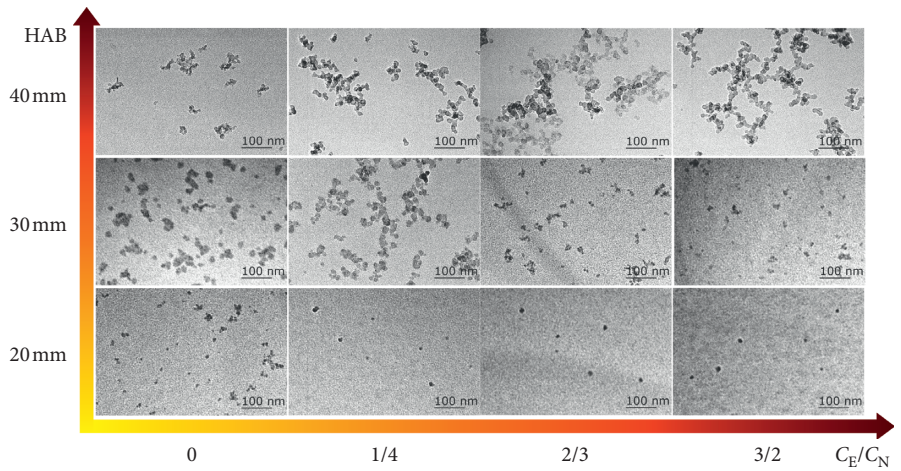

Figure 6: HRTEM image of soot particles in a laminar diffusion flame with *n*-heptane mixed with ethanol.

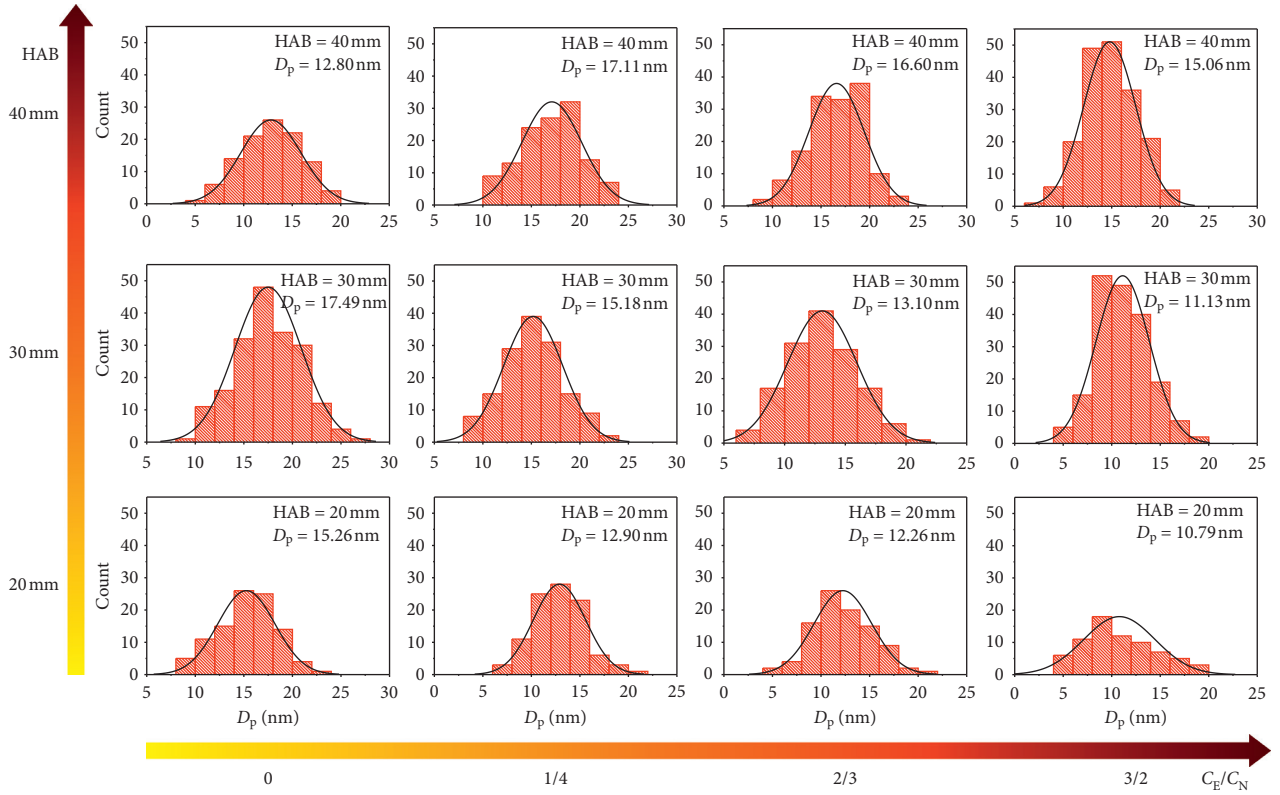

Figure 7: Statistical results of soot particle size in a laminar diffusion flame with *n*-heptane mixed with ethanol.

Table 2: The average particle size of the primary soot at different heights.

HAB (mm)	C_E/C_N			
	0	1/4	2/3	3/2
20	15.26 nm	12.9 nm	12.26 nm	10.79 nm
30	17.49 nm	15.18 nm	13.1 nm	11.13 nm
40	12.8 nm	17.11 nm	16.6 nm	15.06 nm

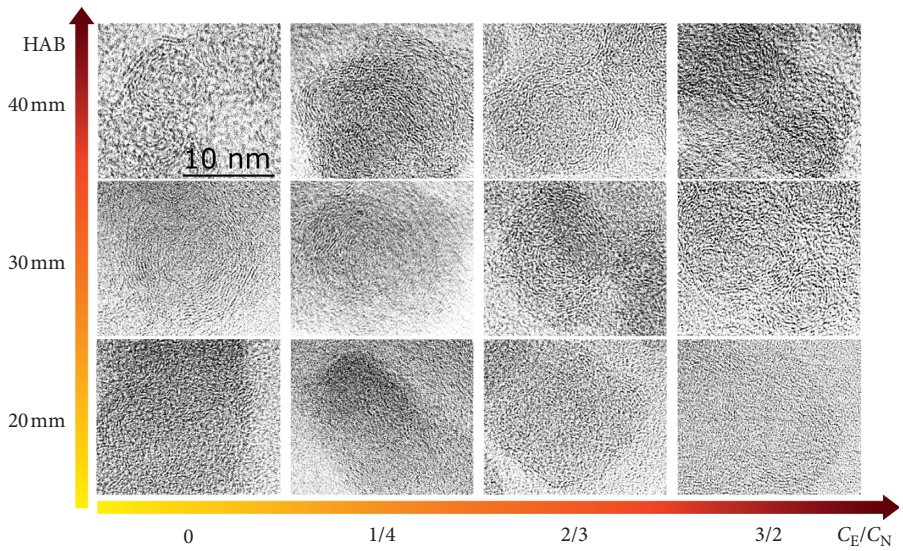

Figure 8: Nanostructure of soot particle in laminar coflow diffusion flames with *n*-heptane mixed with ethanol.

Figure 8 shows HRTEM images of soot magnified by 4×10^5 times along the center of flame at different heights in the ethanol/*n*-heptane flames. From Figure 8, it can be found that the shell structure of soot becomes obvious with the increase of flame height. The addition of ethanol can reduce the aging degree of soot and increase the soot oxidation activity in the high temperature area of the flame (edge and tip location), as the results in [18–20].

4. Conclusions

In this study, the morphological evolution and nanostructure of soot emission in coflow laminar diffusion flames of *n*-heptane blended with ethanol were experimentally studied using thermal swimming probe sampling and HRTEM technology. The main conclusions are as follows:

(1) Under the condition of the same total carbon content, the height of *n*-heptane increased with the increasing ratio of ethanol.

(2) The temperature of the flame center position decreased with the ratio of ethanol blended, while it increased with the ratio at flame edge.

(3) The formation process of soot particles in laminar diffusion flame of *n*-heptane and *n*-heptane/ethanol is similar. However, the soot size at the same height decreases significantly as ethanol increases in the mixed fuels.

Data Availability

All data used to support the findings of this study are included within the article.

Conflicts of Interest

The authors declare that there are no conflicts of interest regarding the publication of this paper.

Acknowledgments

The authors would like to thank the National Natural Science Foundation of China (Grant Nos. 5187827808 and 51676002), Project of Support Program for Outstanding Young People in Colleges and Universities (Grant No. gxyqZD201830) and National Training Program of Innovation and Entrepreneurship for Undergraduates (Grant No. 201910360082) for their financial support of this study.

References

[1] A. P. Rutter, D. C. Snyder, J. J. Schauer, J. DeMinter, and B. Shelton, "Sensitivity and bias of molecular marker-based aerosol source apportionment models to small contributions of coal combustion soot," *Environmental Science & Technology*, vol. 43, no. 20, pp. 7770–7777, 2009.

[2] L. A. Sgro, A. Simonelli, L. Pascarella et al., "Toxicological properties of nanoparticles of organic compounds (NOC) from flames and vehicle exhausts," *Environmental Science & Technology*, vol. 43, no. 7, pp. 2608–2613, 2009.

[3] Z. Lu, D. G. Streets, E. Winijkul et al., "Light absorption properties and radiative effects of primary organic aerosol emissions," *Environmental Science & Technology*, vol. 49, no. 8, pp. 4868–4877, 2015.

[4] M. Brauer, G. Hoek, H. A. Smit et al., "Air pollution and development of asthma, allergy and infections in a birth cohort," *European Respiratory Journal*, vol. 29, no. 5, pp. 879–888, 2007.

[5] R. Lemaire, E. Therssen, and P. Desgroux, "Effect of ethanol addition in gasoline and gasoline-surrogate on soot formation in turbulent spray flames," *Fuel*, vol. 89, no. 12, pp. 3952–3959, 2010.

[6] S. M. Sarathy, P. Oßwald, N. Hansen, and K. Kohse-Höinghaus, "Alcohol combustion chemistry," *Progress in Energy and Combustion Science*, vol. 44, pp. 40–102, 2014.

[7] C. Jin, M. Yao, H. Liu, F. Chia-fon, and J. Ji, "Progress in the production and application of *n*-butanol as a biofuel," *Renewable and Sustainable Energy Reviews*, vol. 15, no. 8, pp. 4080–4106, 2018.

[8] M. Hamdan and B. Jubran, "The effect of ethanol addition on the performance of diesel and gasoline engines," *Dirarst*, vol. 13, no. 10, pp. 229–244, 1985.

[9] I. Aharon, V. Tam, and B. Shaw, "Combustion of submillimeter heptane/methanol and heptane/ethanol droplets in reduced gravity," *Journal of Combustion*, vol. 2013, Article ID 154202, 6 pages, 2013.

[10] Q. Fan, Z. Wang, Y. Qi, and Y. Wang, "Investigating autoignition behavior of *n*-heptane/iso-octane/ethanol mixtures for gasoline surrogates through rapid compression machine measurement and chemical kinetics analysis," *Fuel*, vol. 241, pp. 1095–1108, 2019.

[11] M. D. Li, Z. Wang, Y. Zhao, R. N. Li, and S. Liu, "Experiment study on major and intermediate species of ethanol/*n*-heptane premixed flames," *Combustion Science and Technology*, vol. 185, no. 12, pp. 1786–1798, 2013.

[12] P. Dagaut and C. Togbé, "Experimental and modeling study of the kinetics of oxidation of ethanol-*n*-heptane mixtures in a jet-stirred reactor," *Fuel*, vol. 89, no. 2, pp. 280–286, 2010.

[13] H. J. Curran, P. Gaffuri, W. J. Pitz, and C. K. Westbrook, "A comprehensive modeling study of *n*-heptane oxidation," *Combustion and Flame*, vol. 114, no. 1-2, pp. 149–177, 1998.

[14] R. Seiser, H. Pitsch, K. Seshadri, W. J. Pitz, and H. J. Gurran, "Extinction and autoignition of *n*-heptane in counterflow configuration," *Proceedings of the Combustion Institute*, vol. 28, no. 2, pp. 2029–2037, 2000.

[15] A. Ergut, S. Granata, J. Jordan et al., "PAH formation in one-dimensional premixed fuel-rich atmospheric pressure ethylbenzene and ethyl alcohol flames," *Combustion and Flame*, vol. 144, no. 4, pp. 757–772, 2006.

[16] R. Li, Z. Liu, Y. Han et al., "Investigation into the influence of the ethanol concentration on the flame structure and soot precursor formation of the *n*-heptane/ethanol premixed laminar flame," *Energy & Fuels*, vol. 32, no. 4, pp. 4732–4746, 2018.

[17] T. C. Zannis and D. T. Hountalas, "DI diesel engine performance and emissions from the oxygen enrichment of fuels with various aromatic content," *Energy & Fuels*, vol. 18, no. 3, pp. 659–666, 2004.

[18] F. Yan, L. Xu, Y. Wang, S. Park, S. M. Sarathy, and S. H. Chung, "On the opposing effects of methanol and ethanol addition on PAH and soot formation in ethylene counterflow diffusion flames," *Combustion and Flame*, vol. 202, pp. 228–242, 2019.

[19] Y. Zhang, Y. Li, P. Liu, R. Zhan, Z. Huang, and H. Lin, "Investigation on the chemical effects of dimethyl ether and ethanol additions on PAH formation in laminar premixed ethylene flames," *Fuel*, vol. 256, p. 115809, 2019.

[20] J. H. Stephen and M. W. Anita, "Chemical kinetics of soot particle growth," *Annual Review of Physical Chemistry*, vol. 36, no. 1, pp. 31–52, 1985.

[21] M. L. Botero, D. Chen, S. González-Calera, D. Jefferson, and M. Kraft, "HRTEM evaluation of soot particles produced by the non-premixed combustion of liquid fuels," *Carbon*, vol. 96, pp. 459–473, 2016.

[22] Y. Ying and D. Liu, "Effects of butanol isomers additions on soot nanostructure and reactivity in normal and inverse ethylene diffusion flames," *Fuel*, vol. 205, pp. 109–129, 2017.

[23] Y. Ying and D. Liu, "Nanostructure evolution and reactivity of nascent soot from inverse diffusion flames in CO_2, N_2, and He atmospheres," *Carbon*, vol. 139, pp. 172–180, 2018.

[24] J. Duan, Y. Ying, and D. Liu, "Novel nanoscale control on soot formation by local CO_2 micro-injection in ethylene inverse diffusion flames," *Energy*, vol. 179, pp. 697–708, 2019.

[25] Y. Ying and D. Liu, "Effects of water addition on soot properties in ethylene inverse diffusion flames," *Fuel*, vol. 247, pp. 187–197, 2019.

[26] N. K. Memon, S. D. Tse, J. F. Al-Sharab et al., "Flame synthesis of graphene films in open environments," *Carbon*, vol. 49, no. 15, pp. 5064–5070, 2011.

[27] P. Minutolo, M. Commodo, A. Santamaria, G. De Falco, and A. D'Anna, "Characterization of flame-generated 2-D carbon nano-disks," *Carbon*, vol. 68, pp. 138–148, 2014.

[28] G. Vishwanathan and R. D. Reitz, "Application of a semi-detailed soot modeling approach for conventional and low temperature diesel combustion-part I: model performance," *Fuel*, vol. 139, pp. 757–770, 2015.

[29] P. Lindstedt and L. Maurice, "Detailed kinetic modelling of *n*-heptane combustion," *Combustion Science & Technology*, vol. 107, no. 4–6, pp. 317–353, 1995.

[30] D. Zhou, W. Yang, J. Li, and K. L. Tay, "Simplified fuel cracking process in reduced mechanism development: PRF-PAH kinetic models for combustion and soot prediction," *Fuel*, vol. 182, pp. 831–841, 2016.

[31] H. Wang, R. Deneys Reitz, M. Yao, B. Yang, Q. Jiao, and L. Qiu, "Development of an *n*-heptane-*n*-butanol-PAH mechanism and its application for combustion and soot prediction," *Combustion and Flame*, vol. 160, no. 3, pp. 504–519, 2013.

[32] N. M. Marinov, "A detailed chemical kinetic model for high temperature ethanol oxidation," *International Journal of Chemical Kinetics*, vol. 31, no. 3, pp. 183–220, 2015.

[33] A. Frassoldati, A. Cuoci, T. Faravelli, and E. Rani, "Kinetic modeling of the oxidation of ethanol and gasoline surrogate mixtures," *Combustion Science & Technology*, vol. 182, no. 4–6, pp. 653–667, 2010.

[34] H. Chu, W. Han, W. Cao, M. Gu, and G. Xu, "Effect of methane addition to ethylene on the morphology and size distribution of soot in a laminar co-flow diffusion flame," *Energy*, vol. 166, pp. 392–400, 2019.

[35] W. Han, H. Chu, Y. Ya, S. Dong, and C. Zhang, "Effect of fuel structure on synthesis of carbon nanotubes in diffusion flames," *Fullerenes, Nanotubes and Carbon Nanostructures*, vol. 27, no. 3, pp. 265–272, 2019.

[36] A. Imran, M. Varman, H. H. Masjuki, and M. A. Kalam, "Review on alcohol fumigation on diesel engine: a viable alternative dual fuel technology for satisfactory engine performance and reduction of environment concerning emission," *Renewable and Sustainable Energy Reviews*, vol. 26, pp. 739–751, 2013.

[37] J. Campos-Fernández, J. M. Arnal, J. Gómez, and M. P. Dorado, "A comparison of performance of higher alcohols/diesel fuel blends in a diesel engine," *Applied Energy*, vol. 95, pp. 267–275, 2012.

[38] P. Dagaut, J. Boettner, and M. Cathonnet, "Kinetic modeling of ethanol pyrolysis and combustion," *Journal de Chimie Physique*, vol. 89, pp. 867–884, 1992.

[39] F. Liu, H. Guo, J. Smallwood, and Ö. Gülder, "The chemical effects of carbon dioxide as an additive in an ethylene diffusion flame: implications for soot and NOx formation," *Combustion and Flame*, vol. 125, no. 1-2, pp. 778–787, 2001.

[40] H. Wang, "Formation of nascent soot and other condensed-phase materials in flames," *Proceedings of the Combustion Institute*, vol. 33, no. 1, pp. 41–67, 2011.

[41] A. Raj, M. Sander, V. Janardhanan, and M. Kraft, "A study on the coagulation of polycyclic aromatic hydrocarbon clusters to determine their collision efficiency," *Combustion and Flame*, vol. 157, no. 3, pp. 523–534, 2010.

[42] H. Chu, W. Han, W. Cao, C. Tao, M. Raza, and L. Chen, "Experimental investigation of soot morphology and primary particle size along axial and radial direction of an ethylene diffusion flame via electron microscopy," *Journal of the Energy Institute*, vol. 92, no. 5, pp. 1294–1302, 2019.

[43] B. Guan, Z. Li, D. Han, Z. Huang, and H. Lin, "Size distribution of soot particles in premixed *n*-heptane and methylcyclohexane flames," *Energy & Fuels*, vol. 32, no. 3, pp. 3883–3890, 2018.

[44] M. L. Botero, S. Mosbach, and M. Kraft, "Sooting tendency and particle size distributions of *n*-heptane/toluene mixtures burned in a wick-fed diffusion flame," *Fuel*, vol. 169, pp. 111–119, 2016.

[45] D. Zhang, J. Fang, J. f. Guan et al., "Laminar jet methane/air diffusion flame shapes and radiation of low air velocity coflow in microgravity," *Fuel*, vol. 130, pp. 25–33, 2014.

[46] H. A. K. Shahad and Y. K. A. Mohammed, "Investigation of soot formation and temperature field in laminar diffusion flames of LPG-air mixture," *Energy Conversion and Management*, vol. 41, no. 17, pp. 1897–1916, 2000.